triplet absorption in BCN is inhomogeneously broadened. The efficient energy transfer from the highest energy sites to the lowest energy sites, without the observation of mobility edges, might suggest the absence of Anderson-type localization in this disordered system.

In our previous studies[4] on the tranfer of Eu^{3+} excitation in phosphate glasses at room temperature, we found that the full inhomogeneous profile was recovered uniformly with time following pulsed laser excitation, independent of the laser wavelength used. This suggests that the transfer rate is independent of donor–acceptor energy mismatch. This is expected to be the case when kT is much greater than the inhomogeneous width. In our present system, however, kT is ~ 3 cm^{-1} and the inhomogeneous width is ~ 80 cm^{-1}. Transfer is thus only possible from high- to low-energy sites at this temperature. This is because transfer from a low-energy site to a high-energy site requires the population of phonons which is very small at 4.2 K. For the same reason, the Raman- and Orbach-type phonon-assisted processes[9] would also be unimportant at this low temperature, thus leaving the direct one-phonon emission process as the most probable mechanism for the observed spectral diffusion in this system. For this process, the transfer rate from a donor at site energy E_i can be written as

$$W_{(E_i)} \propto \sum_f c_{if,\omega_{if}} \rho_{f(Ei)} \rho(\omega_{if})(n_{\omega_{if}} + 1) \qquad (1)$$

In this equation c_{if} contains the details of the coupling with phonons required to make up the energy mismatch between the energy of the donor and that of acceptor; $\rho_{f(E_i)}$ is the density of the acceptor states at energy $\leq E_i$ to which energy can be transferred at 4.2 K by the emission of one phonon. (The inhomogeneous profile can be assumed to result from a distribution of sites.) The term n_{if} represents the occupation number of phonons of frequency $\omega_{if} = (E_i - E_f)/\hbar$ and $\rho(\omega_{if})$ is the phonon density of states. At 4.2 K, $(n_{\omega_{if}} + 1)$ is near unity.

Both for small and large energy mismatch, $c_{if,\omega_{if}}\rho(\omega_{if})$ increases with the increase of the energy mismatch (i.e., increase in donor site energy). Furthermore, as the energy of the donor, E_i, increases the density of the acceptors increases (which leads to an increase in the phase space for the energy transfer process). Thus as a result of all these terms, an increase in the transfer rate is expected as the donor energy increases. This fact explains the lack of emission from sites except the ones at the lowest energy. It also explains our spectral diffusion results which show an increase of the emission from the low-energy sites with time upon exciting the higher energy donors.

The observations of the present work are summarized as follows: (i) The spectral profile for the singlet–triplet transition is inhomogeneously broadened by the orientational disorder. (ii) No Anderson type localization is observed for the triplet excitation in this disordered system. (iii) The energy transfer is phonon assisted. (iv) The spectral diffusion rate is site dependent and increases with an increase in the donor energy.

A more quantitative correlation of the theory and the results will require quantitative measurements of the transfer rates of various low-energy sites. Such measurements are in progress and will be reported at a later date.

Acknowledgment. P.P. thanks the donors of the Petroleum Research Fund, administered by the American Chemical Society, and J.M. and M.A.E. thank the Office of Naval Research for financial support of this work.

ARTICLES

Bimolecular Ion–Molecule Addition Reactions in the Gas Phase. Alcohols and Alkoxides

Gary Caldwell and John E. Bartmess*

Department of Chemistry, Indiana University, Bloomington, Indiana 47405 *(Received: March 16, 1981; In Final Form: July 8, 1981)*

In a trapped ICR spectrometer, the larger alcohols ($\geq C_4$) are observed to react with their alkoxides to form $(2M - 1)^-$ cluster ions, following bimolecular kinetics. Alcohols containing additional C–O or C–F bonds also are reactive in this manner. Calculation of RRKM, collisional, and radiative emission rate constants provide a rationale for the observed reactivities. For aliphatic alcohols, the decrease in the unimolecular decomposition rate of the excited cluster ion controls the relative rates. The calculated rates do not provide a clear answer as to whether stabilization of the excited complex is collisional or radiative in nature. The calculations indicate that radiative emission is strongly favored by C–O or C–F bonds.

If an ion and a neutral molecule are brought together, the attractive ion–dipole or ion–induced dipole forces result in the complex being more stable than the separate species. If this process occurs in solution, the solvent can carry away the excess energy of the complex and stabilize it with respect to dissociation. In the gas phase, however, for the chemically activated product complex to survive for long times, it must somehow dispose of its excess energy. In Scheme I, the possible fates of such a complex are presented. After formation at some collision rate k_c, it can

0022-3654/81/2085-3571$01.25/0 © 1981 American Chemical Society

Scheme I

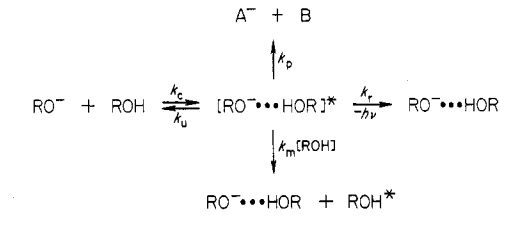

$$k_{calcd}(E) = \frac{k_c(k_r(E) + k_m[ROH])}{k_u(E) + k_r(E) + k_m[ROH] + k_p} \quad (1)$$

revert to reactants unimolecularly at energy-dependent rate k_u, or fall apart to some other set of ion and neutral products at rate k_p, if the excess energy redistributes itself. For the complex to persist in a net addition reaction all or part of the excess energy must be removed, either by collisional stabilization $k_m[M]$, or by radiative emission, k_r. The latter process is highly dependent on the internal energy of the complex. While such addition reactions are well-documented for ion–molecule reactions at the relatively high pressures of chemical ionization mass spectrometers and flowing afterglow spectrometers,[1] only recently have there been reports of clustering occurring at the low pressures of ca.10^{-7}–10^{-6} torr present in the ICR spectrometer. These include electron attachment to fluorinated compounds and a variety of aromatics,[2] silyl cation reactions,[3] formation of proton-bound dimers of ethers,[4] Li^+ association with carbonyl compounds,[5] and CH_3^+ bonding to HCN.[6] The pressure-independent rate constants observed for these reactions indicate that stabilization by radiative emission is the principal, if not sole, method for removal of excess energy from the complex.

In the course of developing the gas-phase acidity scale,[7] it was observed that in the ICR spectrometer the signal due to the M – 1 anion of large ($\geq C_5$) alcohols decreased with time while the ions at $(2M - 1)^-$ correspondingly increased as shown in reaction 2. This was presumed to

$$RO^- + R'OH \rightarrow RO^-\cdots HOR' \quad (2)$$

be due to formation of the hydrogen-bound complex of a neutral alcohol and its alkoxide; double resonance studies indicated that the $(M - 1)^-$ ion was the sole source of the $(2M - 1)^-$ signal. Other alcohols such as the fluorinated ethanols also exhibited such behavior. Such cluster formation has also been reported in the drift ICR; the higher pressures used there, however, prevented determination of the mechanism of formation.[8] In order to further investigate the nature of such association complexes, we have undertaken a study of systematic structure variation in the alcohols which undergo such reactions. While other structure–reactivity studies for bimolecular clustering have been done,[5] the range of structural variation in them has not been large. The present work surveys aliphatic substituents from C_1 to C_{10}, and other heteroatom groups as well. In addition, the use of the symmetrical complexes, involving only R = R′, allows the depth of the well for the complex and therefore the excess energy to remain nearly constant over these large variations in the size and nature of R. As the alcohol becomes a stronger acid and better hydrogen-bond donor, the alkoxide correspondingly becomes a weaker hydrogen-bond acceptor, leveling any changes in the bond strength and well depth. This allows examination of the effect of additional vibrational modes on k_u and k_r without the complications of changing excess energy. For these systems, no other products are seen, so $k_p = 0$.

Experimental Section

Instrumentation. The ICR instrumentation used is similar to that reported in the literature[9] save that it is equipped with a capacitance bridge detector[10] currently utilizing field sweep mode for mass scans. An MKS Baratron Type 146 capacitance manometer was used in the 10^{-6}–10^{-5}–torr range to calibrate the Granville-Phillips Type 270 ionization gauge controller with a Huntington Mechanical Labs Bayard-Alpert gauge. Mass scans were normally done at 153.56 kHz, except when masses beyond the 14-kG range of the magnet required a lower (typically 100 or 75 kHz) frequency. Rate constants were obtained at as high a magnetic field as practical to minimize collisional ion loss from the cell. We obtain a rate constant for the reaction $CH_4^{+\cdot} + CH_4 \rightarrow CH_5^+ + CH_3\cdot$ of $(1.06 \pm 0.11) \times 10^{-9}$ cm^3 molecule^{-1} s^{-1}, in good agreement with the average literature value[11] of $(1.11 \pm 0.04) \times 10^{-9}$ cm^3 molecule^{-1} s^{-1}.

The temperature gradients across the cell which interfered with exact temperature assignments previously[7] have been largely eliminated by redesign. The rhenium filament is now supported on tungsten rods out of direct contact with the cell trapping plate.[12] Even at filament currents in excess of 3.5 A, the cell trapping plate rises no more than 5 °C above ambient. Data were normally collected with the ionization gauge off, to avoid pyrolysis problems.[38]

Chemicals. Chemicals were either obtained commercially or prepared as described in ref 7. All samples were purified by distillation, sublimation, or preparative GC before use, and were degassed by several freeze–pump–thaw cycles on the ICR foreline before being admitted into the main vacuum system.

Infrared Spectra. These were obtained in absorption mode on a Digilab FTS-15C FT IR spectrometer. The gas cells were 15 cm long; data were collected at the alcohols' vapor pressures at 28 °C, using a varying number of scans depending on sample pressure. Integration was performed by the standard Digilab routine.

Results

Experimental Rate Constants. The M – 1 anions of the various alcohols in Table I were generated by proton transfer to methoxide, formed by thermal electron impact on methyl nitrite. The methyl nitrite was at a pressure

(1) Lau, Y. K.; Saluja, P. P. S.; Kebarle, P. *J. Am. Chem. Soc.* **1980**, *102*, 7429–33. Yamdagni, R.; Kebarle, P. *Ibid.* **1971**, *93*, 7139–43. Arshadi, M.; Kebarle, P. *J. Phys. Chem.* **1970**, *74*, 1483–5. Bohme, D. K.; Mackay, G. I. *J. Am. Chem. Soc.* **1980**, *102*, 407–8. Mackay, G. I.; Bohme, D. K. *Ibid.* **1980**, *102*, 327–9.

(2) Woodin, R. L.; Foster, M. S.; Beauchamp, J. L. *J. Chem. Phys.* **1980**, *72*, 4223–7. Foster, M. S.; Beauchamp, J. L. *Chem. Phys. Lett.* **1975**, *31*, 482–6.

(3) Murphy, M. K.; Beauchamp, J. L. *J. Am. Chem. Soc.* **1976**, *98*, 5781–8. Allen , W. N.; Lampe, F. W. *Ibid.* **1977**, *99*, 2943–8, 6816–22.

(4) Bomse, D. S.; Beauchamp, J. L. *J. Am. Chem. Soc.* **1980**, *102*, 3967–9.

(5) Woodin, R. L.; Beauchamp, J. L. *Chem. Phys.* **1979**, *41*, 1–9.

(6) McEwan, M. J.; Anicich, V. G.; Huntress, W. T.; Kemper, P. R.; Bowers, M. T. *Chem. Phys. Lett.* **1980**, *75*, 278–82.

(7) Bartmess, J. E.; McIver, R. T., Jr. "Gas Phase Ion Chemistry", M. T. Bowers, Ed.; Academic Press: New York, 1979; Vol. 2, Chapter 11. Bartmess, J. E.; Scott, J. A.; McIver, R. T., Jr. *J. Am. Chem. Soc.* **1979**, *101*, 6046–56.

(8) Dawson, J. H. J.; Jennings, K. R. *Int. J. Mass Spectrom. Ion Phys.* **1977**, *25*, 47–53.

(9) McIver, R. T., Jr. *Rev. Sci. Instrum.* **1970**, *41*, 555–8. *Ibid.* **1978**, *49*, 111–8. McIver, R. T., Jr. "Ion Cyclotron Resonance Spectrometry", Hartmann, H.; Wanczek, K.-P., Ed.; Springer-Verlag: Berlin, 1978; 97–135.

(10) Hunter, R. L.; McIver, R. T., Jr. *Chem. Phys. Lett.* **1977**, *49*, 577–82.

(11) Huntress, W. T.; Laudenslager, J. G.; Pinizzoto, R. F. *Int. J. Mass. Spectrom. Ion Phys.* **1974**, *13*, 331–41.

(12) Wren, A. G.; Gilbert, P.; Bowers, M. T. *Rev. Sci. Instrum.* **1979**, *49*, 531–6.

TABLE I: Formation of $(2M - 1)^-$ Cluster Ions of Alcohols in a Trapped ICR Spectrometer

ROH	$RO^-\cdots HOR$ formation[a]	k,[b] cm^3 $molecule^{-1}$ s^{-1}
MeOH	no	
EtOH	no	
n-PrOH	no	
i-PrOH	no	
n-BuOH	tr	
i-BuOH	tr	
s-BuOH	tr	
t-BuOH	tr	
$EtC(Me)_2OH$	yes	
t-$BuCH_2OH$	yes	8.0×10^{-11}
t-BuCH(Me)OH	yes	7.5×10^{-11}
t-BuCH(Et)OH	yes	1.2×10^{-10}
t-BuCH(*i*-Pr)OH	yes	1.2×10^{-10}
$(t\text{-Bu})_2CHOH$	yes	1.4×10^{-10}
CF_3CH_2OH[c]	yes	6.6×10^{-11}
$(CF_3)_2CHOH$[c]	yes	
c-$C_6H_{11}OH$	yes	
c-$C_5H_5CH(Me)OH$	yes	
$PhCH_2OH$	yes	
$PhCH_2SH$	no	
$(i\text{-Pr})_2NH$[d]	no	

[a] no = no $(2M - 1)^-$ seen, quenched or unquenched.[13,14] tr = $(2M - 1)^-$ seen unquenched, intensity less than that of $(M - 1)^-$. yes = $(2M - 1)^-$ seen at long times, quenched. [b] ±20%, see text. [c] A small amount [5–8% of $(2M - 1)^-$ intensity, unquenched] of $(3M - 1)^-$ is seen. [d] NH_2^- as primary base.

of $<1 \times 10^{-7}$ torr, the alcohols at pressures varying from 2×10^{-7} to 4×10^{-6} torr. Under these conditions the M – 1 anion is observed to form in the first few hundred milliseconds, then reacts away as the 2M – 1 ion forms over hundreds of milliseconds to seconds. Analysis of time plots of these ions' abundances as pseudo-first-order data by linear regression gives the rate constants in the last column of Table I. The values for the disappearance of the (M – 1) and appearance of the $(2M - 1)^-$ agree to within 20% typically with $r > 0.990$. The principal source of error in the rate constants is the uncertainty in the neutral pressures, due to the necessity of calibrating the ionization gauge against the capacitance manometer at the extreme lower end of the latter's range, 10^{-6}–10^{-5} torr. We estimate the absolute accuracy of the rate constants as ±20% as a result, though their accuracy relative to one another is probably better. For those alcohols where only a qualitative indication is given, that represents observation of an appreciable $(2M - 1)^-$ peak in the unquenched mode.[13] Analysis of the kinetics that operate in the unquenched mode[14] indicates that the ratio of the $(2M - 1)^-$ to $(M - 1)^-$ peaks should be roughly equal to the ratio of the clustering rate to the collisional loss rate from the cell. The latter is approximately 5×10^{-12} cm^3 $molecule^{-1}$ s^{-1}, providing a semiquantitative measure of the slower clustering rates. The clustering of the C_4 alcohols by this method is close to the collisional loss rate, while the C_5 and larger molecules are faster. There is no evident dependence of the observed rate constants on pressure as is shown in Figure 1. Both the scatter and intercept of such plots are within the 20% uncertainty of the individual values for all alcohols investigated. No correction for collisional ion loss from the cell is included in the rate constant determinations since even the slowest measured reactions are an order of magnitude faster than the loss rate. The ions 46^- and 60^- from CH_3ONO do not perturb the cluster ions' abundance, as shown by double resonance.

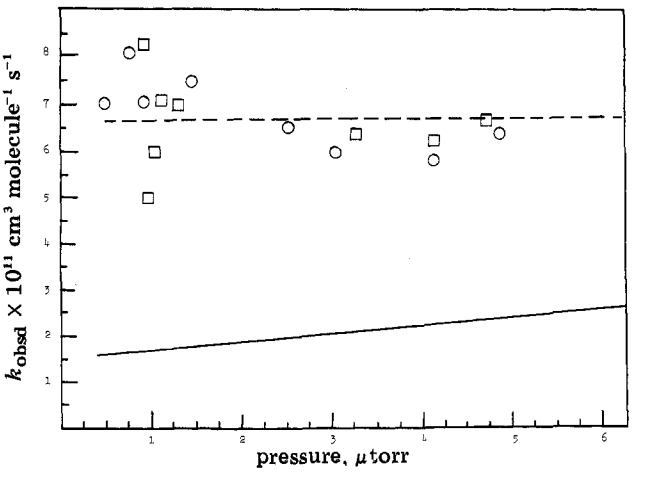

Figure 1. Pressure dependence of the rate constant (cm^3 $molecule^{-1}$ s^{-1}) for clustering of CF_3CH_2OH. Circles denote the disappearance of the (M – 1) and squares denote the appearance of the (2M – 1). The dashed line represents the mean of the data points. Solid line is pressure dependence based on eq 12.

Theoretical Calculations. While the lack of pressure dependence for the observed rate constants is indicative that the stabilization is primarily radiative in nature, the low concentration of ions in the ICR (ca. $10^6/cm^3$) makes direct detection of the photons difficult.[15] To provide further support for the proposed mechanism, we have calculated what the overall rate constant of Scheme I should be as a function of structure and pressure, in a manner similar to that of Woodin and Beauchamp.[5] While the methods employed are not exact, any consistent trends in the calculated vs. experimental rate constants with structure variation should provide support for the proposed mechanism.

The collisional rate constant, k_c, is evaluated by the ADO method of Su and Bowers.[16] This method is strictly valid only for thermalized ions and neutrals. The neutral reactants are certainly thermal due to their many collisions with the vacuum system's walls before entering the ICR cell. The primary ions generated by electron impact in this work may have some internal excess energy;[17] however, since the electron energy involved is less than 1 eV, this is at most a few kilocalories per mole.

While the enthalpy of proton transfer (up to 14.8 kcal/mol here[7]) can technically be deposited in the product alkoxide ion, it is expected that much of the excess enthalpy will remain in the newly formed bond in the neutral methanol product, since the proton transfer is a near-resonant process.[7,18] Excess ion translational energy is rapidly lost in the ICR cell due to neutral collisions and to coupling of the ions' motion, via image currents, with the external circuitry. We thus believe that the collision reaction involves near-thermal particles. The rate constant for collisional stabilization of the excited intermediate, k_m, is similarly calculated as an ADO rate constant[16] by using the mass of the cluster ion.

(13) Hunter, R. L.; McIver, R. T., Jr. *Anal. Chem.* **1979**, *51*, 699–704.
(14) Bartmess, J. E.; Caldwell, G. Accepted for publication in *Int. J. Mass Spectrom. Ion Phys.*

(15) Bierbaum, V. M.; Ellison, G. B.; Futrell, J. H.; Leone, S. R. 25th Annual Conference on Mass Spectrometry and Allied Topics, Washington, DC, 29 May–3 June 1977, paper RB5. Mauclaire, G.; Marx, R.; Van de Runstraat, C.; Fenistein, S. *Int. J. Mass Spectrom. Ion Phys.* **1976**, *22*, 339–58.
(16) (a) Su, T.; Bowers, M. T. *J. Chem. Phys.* **1973**, *58*, 3027–37. (b) *Int. J. Mass Spectrom. Ion Phys.* **1973**, *12*, 347–56. (c) Su, T.; Su, E. C. F.; Bowers, M. T. *J. Chem. Phys.* **1978**, *69*, 2243–50.
(17) Riveros, J. M.; Briscese, S. M. J. *J. Am. Chem. Soc.* **1975**, *97*, 230–1. Sullivan, S. A.; Beauchamp, J. L. *Ibid.* **1977**, *99*, 5017–22.
(18) McMahon, T. B.; Beauchamp, J. L. *J. Phys. Chem.* **1977**, *81*, 593–8. McDonald, J. D. *Annu. Rev. Phys. Chem.* **1979**, *30*, 29–50.

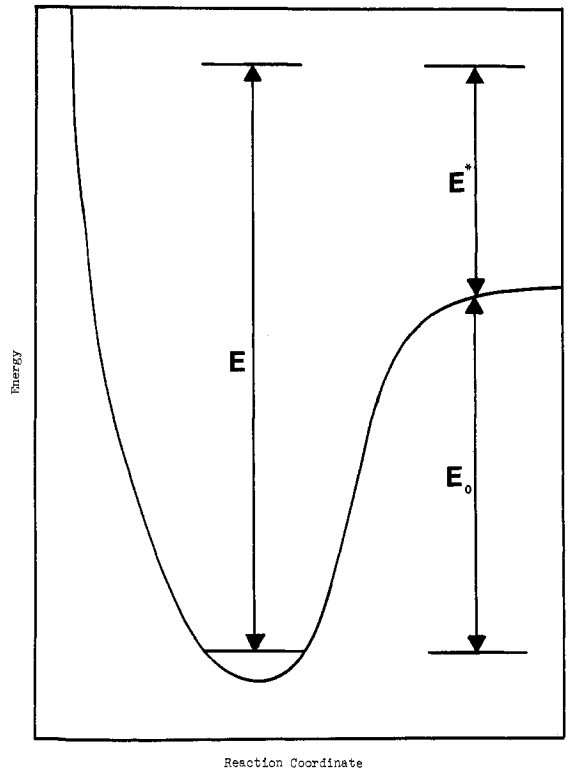

Figure 2. Potential surface for the clustering of alcohols.

RRKM theory[19] is used to evaluate the unimolecular rate constant, $k_u(E)$, for decomposition of the intermediate back to reactants. Equation 3 expresses this rate as a

$$k_u(E) = \frac{pG^*(E - E_0 - J^2(B^\ddagger - B))}{hN(E)} \quad (3)$$

function of the sum of states G^* up to energy E^* ($= E - E_0 - J^2(B^\ddagger - B)$) for the transition state for separation, the density of states $N(E)$ for the complex in the well, and a statistical factor p for the possible paths to decomposition (here $p = 2$). $B^\ddagger$ is the rotational constant for the transition state (loose complex) and B is for the tight complex. J is, to a first approximation, taken as $(E_{rot}/B)^{1/2}$. The relationship of the various energies used is shown in Figure 2, where E_0 is the depth of the well for the complex relative to the transition state for separation. This well depth has not been directly determined for any of the systems investigated here; however, eq 4 has been shown to correlate

$$-\Delta H^\circ_{298} = 0.066\Delta H^\circ_{acid}(AH) \quad (4)$$

such cluster bonding strengths for a wide variety of localized anions with good hydrogen-bond donors, including $HO^-\cdots HOH$.[20] Preliminary investigations in these laboratories by means of exchange equilibria such as (5)

$$MeO^-\cdots HOMe + EtOH \rightleftarrows EtO^-\cdots HOMe + MeOH \quad (5)$$

indicate that it holds for alcohol systems as well, to at least ±2 kcal/mol.[35] The well depth predicted by eq 4 changes only slightly with acidity, from −25.0 to −24.0 kcal/mol as ΔH°_{acid} changes over 15 kcal/mol and the number of oscillators in the complex rises from 28 to 172. There is a small difference between E_0 and ΔH°_{298} from eq 4, but, as will be seen below, the overall calculation is relatively insensitive to changes in well depth of 1–2 kcal/mol, especially in relative rates.

The transition state for breakup of the complex is taken from the Gorin model[21] as the orbiting radius in ADO theory, ranging from 7 to 9 Å between the oxygens here.[16] Direct count was used to obtain sums of states up to an energy where the Whitten–Rabinovitch method[19] provided a good approximation of these. In the interest of computer time the approximation was used at higher energies. The transition was taken at 10 kcal/mol for $MeO^-\cdots HOMe$, down to 3 kcal/mol for the C_5 and larger systems. Since experimental spectroscopic data are not available for the alkoxides or the complexes, we assume that the vibrational frequencies of the R groups in $RO^-\cdots HOR$ and RO^- are not changed from those in ROH.[22] Taking the complex as assymmetric, the O–H and $O^-\cdots H$ stretching and bending frequencies are calculated from a normal-mode analysis[23] by using parameters from Jorgenson.[24] The $O^-\cdots H$ stretch at 1660 cm^{-1} is taken as the reaction coordinate. The $O-H\cdots{}^-O$ bond lengths and angles for the calculated methoxide–methanol complex were used for all alcohols.

The rate constants for radiative emission from the excited complex are evaluated by means of eq 6 by the method of Dunbar.[26] $P^i_n(E)$ is the probability that the nth level of the ith vibrational mode is populated at some total energy E, and $A^i_{n,n-1}$ is the Einstein coefficient for spontaneous emission of a photon from that level. It is assumed that the selection rule $\Delta n = 1$ applies. The Einstein coefficient for an excited state can be related to that for the $1 \rightarrow 0$ state in the harmonic approximation by eq 7, and that to the observed IR integrated band intensity α^i by eq 8.[26]

$$k_r(E) = \sum_i (\sum_n P^i_n(E) A^i_{n,n-1}) \quad (6)$$

$$A^i_{n,n-1} = nA^i_{1,0} \quad (7)$$

$$A^i_{1,0} = 8\pi\nu_i^2\alpha^i \quad (8)$$

The probability function $P^i_n(E)$ is assumed to be a Boltzmann distribution as in eq 9, but one considerably hotter than room temperature due to the fact that the tight complex is formed in a chemically activated manner. The assumption of a Boltzmann distribution is reasonable considering the strong ion–dipole interactions that exist as the collision occurs and the tight complex is formed. The internal temperature T_{int} is evaluated at each energy in the well by means of eq 10.[27] In terms of statistical mechanics eq 10 is equivalent to eq 11 used by other

$$P^i_n(E) = \frac{\exp(-nh\nu_i/kT_{int})}{\sum_n \exp(-nh\nu_i/kT_{int})} \quad (9)$$

$$E = \sum_i \frac{Nh\nu_i}{\exp(h\nu_i/kT_{int}) - 1} \quad (10)$$

$$E = H_T^\circ - H_0^\circ - 4RT \quad (11)$$

(19) Robinson, P. J.; Holbrook, K. A. "Unimolecular Reactions"; Wiley: New York, 1972.
(20) Yamdagni, R.; Kebarle, P. K. *J. Am. Chem. Soc.* **1971**, *93*, 139–43.
(21) Gorin, E.; Kauzman, W.; Walter, J. Eyring, H. *J. Chem. Phys.* **1939**, *7*, 633–45.
(22) Sverdlov, L. M.; Kovner, M. A.; Krainov, E. P. "Vibrational Spectra of Polyatomic Molecules"; Wiley: New York, 1970. Green, J. H. S. *Trans. Faraday. Soc.* **1963**, *59*, 1559–63. Beyon, E. T., Jr.; McKetta, J. *J. Phys. Chem.* **1963**, *67*, 2761–5. Venkateswarea, K.; Mariam, S. *Acta Phys. Austriaca* **1962**, *15*, 362–70. Barnes, A. J.; Hallan, A. E.; Jones, D. *Proc. R. Soc. London, Ser. A.* **1973**, *335*, 97–111. For the larger alcohols not found in the literature, standard bond frequencies from the above references were used.
(23) McIntosh, D. F.; Peterson, M. R. Program 342, Quantum Chemistry Program Exchange, Indiana University, Bloomington, IN 47405.
(24) Jorgenson, W. *J. Comp. Chem.* **1981**, *2*, no. 1, 7–11.
(25) Forst, W. "Theory of Unimolecular Reactions"; Academic Press: New York, 1973; pp 206–8.
(26) Dunbar, R. C. *Spectrochim. Acta, Part A* **1975**, *31*, 797–800.
(27) McQuarrie, D. H. "Statistical Mechanics"; Harper and Row: New York, 1976; p 156.

TABLE II: Calculated Rate Constants for the Processes in Scheme I

ROH	$10^9 \cdot k_{ADO}$[a]	k_m[ROH][b]	$\langle k_u \rangle_{ss}$[c]	$\langle k_r \rangle_{ss}$[d]	k_{calcd}[e]	E_0[f]	T_{int}[g]
MeOH	1.98	6.0	5.3×10^7	20.5	1.0×10^{-15}	25.0	1180
EtOH	1.82	5.5	1.9×10^5	12.0	1.6×10^{-13}	24.8	853
i-PrOH	1.72	5.3	6.1×10^3	6.1	3.2×10^{-12}	24.7	693
t-BuOH	1.66	5.1	619	5.1	2.7×10^{-11}	24.6	602
t-$BuCH_2OH$	1.61	4.9	111	5.0	1.3×10^{-10}	24.5	536
t-BuCH(Me)OH	1.57	4.8	33	4.3	3.4×10^{-10}	24.5	486
t-BuCH(Et)OH	1.54	4.7	17	4.4	5.5×10^{-10}	24.4	449
t-BuCH(*i*-Pr)OH	1.52	4.6	2	4.2	7.4×10^{-10}	24.3	419
$(t\text{-Bu})_2CHOH$	1.50	4.6	0.05	3.9	8.0×10^{-10}	24.2	399
CF_3CH_2OH	1.53	4.7	3.5×10^3	33.2	1.6×10^{-11}	24.0	715

[a] Reference 16, cm^3 $molecule^{-1}$ s^{-1}. [b] Collisional stabilization, expressed as a pseudo-first-order rate constant at [ROH] = 1×10^{-7} torr, in s^{-1}. [c] Unimolecular dissociation rate constant at steady-state abundance, s^{-1} (ref 25). [d] Radiative emission rate constant at steady-state abundance, s^{-1} (ref 25). [e] Calculated rate constant for formation of $(2M - 1)^-$, eq 1, cm^3 $molecule^{-1}$ s^{-1}, [ROH] = 1×10^{-7} torr. [f] Well depth, from eq 4, kcal/mol. [g] Internal temperature at $E = E_0$, from eq 10, K.

workers in the calculation of radiative rates.[5,26] In those cases, however, the ion involved was a molecular cation[26] or a neutral with an atomic ion attached.[5] These are sufficiently similar to the neutral molecule that their experimental heat content function could be taken as a good approximation to that of the neutral's. In the present study, no such appropriate neutral exists, requiring use of eq 10. T_{int} is found to vary from 1180 K for $CH_3O^-\cdots HOCH_3$ to 399 K for $(t\text{-Bu})_2CHO^-\cdots HOCH(t\text{-Bu})_2$ at a well depth of ca. 25 kcal/mol. This is consistent with the same amount of energy in all cases being distributed into more modes in the larger systems, resulting in lower internal vibrational temperatures.

In practice $k_r(E)$ is obtained by using the frequencies for the excited complex described in the above section on the unimolecular decomposition rate. Integrated band intensities are assumed to be the same in the complex as in the neutral alcohols for those vibrations in the R groups that are similarly transferred. These are obtained from tabulated intensities,[28] or by integration of bands in the experimental absorption spectra. For the five estimated frequencies associated with the hydrogen-bonded site, absorption intensities are not available. For the bends, torsions, and the $-O^-\cdots H-$ stretch, the frequencies are sufficiently low that the ν_i^2 dependence in eq 8 allows us to neglect them. Lacking other data, the O–H stretch intensity is taken as that of the free alcohol.

Combining eq 6–10 allows $k_r(E)$ to be calculated. Values of $k_r(E)$ are given in Table II at the steady-state abundance.[25] To obtain a total calculated rate constant for appearance of the stabilized complex, eq 1, with eq 3 and 6 substituted in, is integrated over the Boltzmann energy distribution[5] in the complex according to eq 12. Values

$$k_{calcd} = \int_{E_0}^{\infty} k_{calcd}(E) \times \left[\frac{N(E - E_0) \exp(-(E - E_0)/kT)}{\int_0^{\infty} N(E - E_0) \exp(-(E - E_0)/kT)\, dE} \right] dE \quad (12)$$

are given in Table II. In practice, a summing technique in 50 cal/mol steps is employed.

Discussion

Examination of Table II shows that the calculated rate constants parallel the trend of the experimental rate constants, although the calculated values are 2–6 times larger. The main factor controlling the relative clustering rates for the aliphatic alcohols is k_u, which decreases by an order of magnitude or more for each additional carbon atom present. This can be rationalized qualitatively; if the number of vibrations available for energy to distribute itself in increases, while total excess energy remains constant, it is statistically less likely that all of the energy will find itself in the hydrogen bond stretch at the same time to give it sufficient energy to rupture. Similarly, the collision and radiative rate constants decrease with increasing aliphatic alcohol size. The trend in the collision rate is due mostly to the inverse reduced mass dependence of ADO rates.[16] The radiative emission rate constants are of the millisecond lifetimes expected.[26,29] As with k_u, the trend of decreasing rate constant k_r with increasing structure complexity is explicable in terms of a constant amount of energy spread over a varying number of vibrational modes. The larger the molecule, the less energy is present in any one vibration, and the less likely that mode is to emit a photon.

The greater sensitivity of k_u to structural change compared to k_c, k_m, or k_r is evident in Table II: nine orders of magnitude compared to less than one. The unimolecular decomposition is clearly the controlling factor in the observed rates in this work. The collision and radiative stabilization rate constants are not only smaller and less sensitive to structure than k_u, but their presence in both the numerator and denominator of eq 1 makes k_{calcd} much less sensitive to changes in their values than to k_u.

The calculations predict a 25–70% increase in rate constant as the neutral pressure is increased from 10^{-7} to 10^{-6} torr. As mentioned before, such a trend is not observed experimentally. An examination of possible sources of error in the model for the calculations is useful here. Equation 1 assumes that every collision of excited complex with a neutral serves to stabilize the hydrogen-bonded complex. Efficiencies of less than unity for collisional stabilization of cationic proton-bound dimers of Me_3N have been observed.[30] Similar results are seen for removal of excess energy of neutral systems.[31] Such inefficiency would reduce the sensitivity of k_{calcd} to pressure.

The calculation of the radiative rate will also tend to err on the low side of the true value, since terms were not included for the low-frequency vibrations of the $O^-\cdots H-O$ region. We lack integrated absorption coefficients for these, and assume that the wavelength dependence of k_r will make these vibrations of minor importance and relatively constant for all alcohols. The net effect of the above errors will be to overestimate the relative importance of collisional stabilization relative to radiative stabilization

(28) Wexler, H. S.; *Spectrochim. Acta, Part A* **1965**, *21*, 1725–42.
(29) Jasinski, J. M.; Brauman, J. I. *J. Chem. Phys.* **1980**, *73*, 6191–5.
(30) Cates, R. D.; Bowers, M. T. *J. Am. Chem. Soc.* **1980**, *102*, 3994–6.
(31) Carr, R. W., Jr. *Chem. Phys. Lett.* **1980**, *74*, 437–41.

in the calculations, in agreement with the experimental data.

Another possible source of error involves use of eq 4 to predict E_0. In the vicinity of the values used, the calculated rate increases by 30% for every kilocalorie per mole increase in the well depth. As mentioned above, no experimental data on E_0 are available for alcohol–alkoxide systems, save by interpolation with eq 4. MO calculations[24] at the 4-31G* level indicate that $CH_3O^-\cdots HOCH_3$ is bound only 70% as tightly as $HO^-\cdots H_2O$, while eq 4 predicts 97%. If the MO calculations are even qualitatively right, our calculated rates would be slowed by at least an order of magnitude, though the relative rates would not be appreciably altered. The relative k_{calcd} values for the various alcohols vary only by a factor of 3–5 over a 5 kcal/mol change in well depth. The neglect of conservation of angular momentum likewise could be a source of error. At low temperatures, such inclusion can reduce rates for reaction schemes like the present system by up to an order of magnitude. At room temperature, the effect is smaller, however.[32]

It is tempting to assume that the calculated rates, since they parallel the experimental values, may be scaled to them so that rate constants can be estimated for those small alcohols which were not observed to cluster on the ICR time scale. The problem with this lies in the nature of the errors in the calculated rate constants. There is considerable uncertainty in the exact freqeuncies for the complex obtained from normal-coordinate analyses. The higher frequencies (above ca. 600 cm^{-1}) can be checked against experimental data; the lower frequencies, especially those for the $O^-\cdots H-O$ region, both are much less certain and cannot be checked, lacking experimental data. For the larger systems, most of the frequencies contributing to $k_u(E)$ are the well-known ones. For systems like $CH_3O^-\cdots HOCH_3$, however, the lower modes are a much larger proportion of the total, and the unimolecular rate is much less reliable than for the larger systems. Since k_u is the principal determinant of the overall rate, we believe no better than order of magnitude significance can be attached to the calculated values for the C_1–C_3 alcohols.

Trifluoroethanol clusters much more rapidly than does its aliphatic analogue with the same number of vibrations, ethanol. Table II reveals this is a combination of a reduction in k_u and an increase in k_r. The decrease in k_u is due to the decrease in frequency for C–F modes compared to C–H. This decreases both the sum and density of states in eq 3, but the latter is much more sensitive to such changes, since at a given energy the loose complex at the transition state is much lower in its manifold than the tight complex in the well is.

The increase in k_r requires analysis of the various factors in eq 6. At a fixed T_{int} if $A^i_{1,0}$ is set to unity for all vibrations, then the frequency dependence of k_r can be found as given in Figure 3, a plot of $\nu_i^2\sum_n P_n{}^i(E)$ against ν_i. The ν_i^2 term favors emission from the higher frequencies while the $\sum_n P_n(E)$ term favors the lower frequencies, since more levels are occupied up to any given energy. This produces a maximum in the intermediate frequency ranged around 1200 cm^{-1}, with less emission, all other things equal, from higher or lower frequencies. Thus a C–F stretch at 1200 cm^{-1} is much better at emitting a photon than C–H at 3000 cm^{-1}, assuming equal intensities. As T_{int} increases, this maximum shifts to slightly higher frequency, broadens, and increases in intensity considerably, as shown in Figure 3. Figure 4, where the same function is plotted against temperature for selected frequencies, clearly reveals the importance of frequency. At room temperature, all emission is weak, but the lowest frequency modes predominate. The absolute intensity as well as preference for intermediate frequencies increases with increasing internal temperature

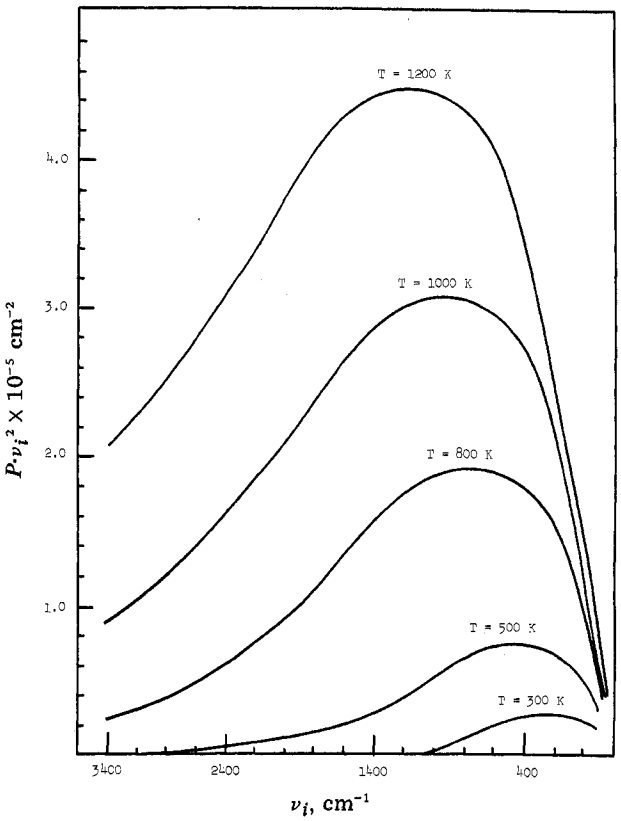

Figure 3. Frequency dependence of the radiative emission rate constant, with $A^i_{0,1} = 1$, for selected internal temperatures.

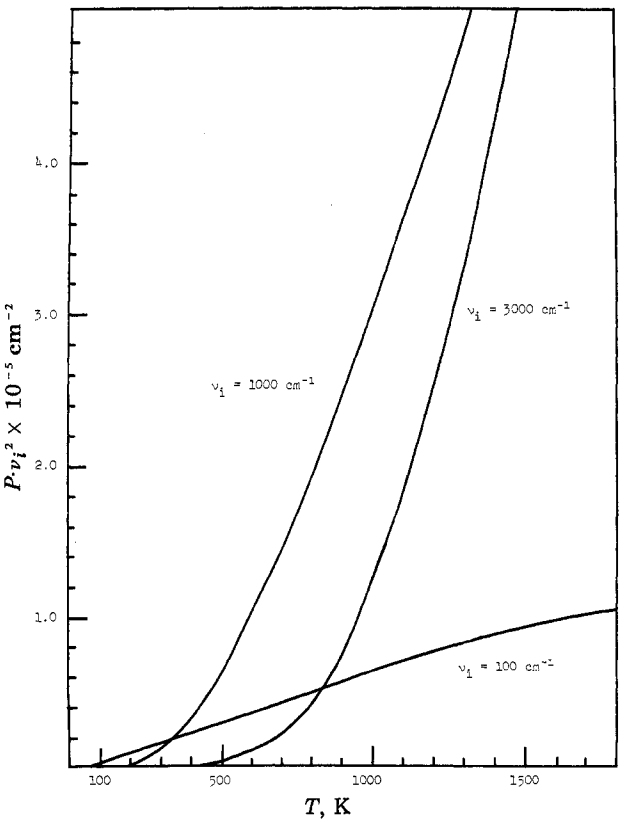

Figure 4. Internal temperature dependence of the radiative emission rate constant, with $A^i_{0,1} = 1$ for selected frequencies.

(32) Herbst, E. *Astrophys. J.* **1980**, *241*, 197–9.

in the range accessible by chemical activation. At sufficiently high temperatures, it appears that C–H bonds will be preferred over C–F; however, at such energies, electronic states become accessible. The net effect is that in our systems, both the frequency and very strong $A^{i}_{0,1}$ for C–F greatly increases radiative emission.

Other systems provide further support for this analysis. Only a small amount of clustering is seen for 1-butanol in the ICR, while 2-methoxyethanol does so readily. This is presumably similar to the fluorinated alcohols: a C–O stretch is both intense and in the right frequency range to increase k_r and decrease k_u compared to a C–C bond. We note that nearly all the reported cases of bimolecular clustering in the laboratory involve compounds with C–O bonds, or the S–F bond at comparable frequency.[2-5] Benzyl mercaptan does not cluster with its mercaptide, while benzyl alcohol is comparable in clustering rate to the largest alcohols here. The C–S stretch, while at 650 cm^{-1} is lower than the C–O stretch,[33] nevertheless is still at a favorable frequency from Figure 3. The weak absorbance of the S–H stretch relative to O–H may be a factor here; however, the well depth E_0 is also important. The shallower the well, the slower the overall reaction. It is well-known that thiols are much weaker at hydrogen bonding in solution than alcohols.[34] If $RS^{-}\cdots HSR$ bond was only 2.5 kcal/mol weaker than predicted by eq 3, the clustering rate would be slower than our time window in the ICR. We are currently measuring such bond strengths by an equilibrium method.[35] Diisopropylamine does not cluster with its amide, while C_6 alcohols do. The weakness of the C–N stretch[33] may be the cause of this.

There has been considerable recent interest in advancing the analytical capability of ICR spectrometry due to its instrumental simplicity, high mass resolution,[36] and capability for use of selective polar reagent gases in chemical ionization mode.[37] The problem with the use of polar reagent gases in conventional chemical ionization mass spectrometry is the termolecular clustering of such polar molecules onto ions at the reagent pressures of ca. 1 torr. This results in a variety of ions for each sample, rather than the single peak desired. At the low pressures used in the trapped ICR spectrometer, such clustering is much less likely to occur.[37] The recent developments in ICR have involved using lower pressures and higher magnetic fields. These are necessary to increase mass resolution, which goes as the reciprocal of pressure, while maintaining total collision number to effect chemical ionization, since trapping time is a function of the square of the magnetic field. The present work indicates that reagent plus sample cluster ions can still form no matter how low the pressure. Both sample ionization and clustering are bimolecular reactions at low pressure. If the simplest possible mass spectrum is desired, it would be advantageous to avoid the use of reagent gases containing C–O or C–F moieties. Conversely, the presence of cluster ions may be indicative of such structural features in the sample.

Acknowledgment. We thank the Research Corporation and the National Institutes of Health, Grant GM-27743-01, for support of this work. We are grateful to Professors G. E. Ewing and C. S. Parmenter, and Mr. Rex Pendley for helpful discussions.

(33) Silverstein, R. M.; Bassler, G. C. "Spectrometric Identification of Organic Compounds"; Wiley: New York, 1967; 2nd ed, pp 86–100.
(34) Pimentel, G. C.; McClellan, A. L. "The Hydrogen Bond"; W. H. Freeman: San Francisco, 1960. Vinogradov, S. N.; Linell, R. H. "Hydrogen Bonding"; Van Nostrand-Reinhold: New York, 1971.
(35) McIver, R. T., Jr.; Scott, J. A.; Riveros, J. M. *J. Am. Chem. Soc.* **1973**, *95*, 2706–8. Bartmess, J. E.; Caldwell, G. 29th Annual Conference on Mass Spectrometry and Allied Topics, Minneapolis, MN, May 24–29, 1981, Paper MPAIO.
(36) Comisarow, M.; Marshall, A. G. *Chem. Phys. Lett.* **1974**, *25*, 282–3. Comisarow, M. In "Ion Cyclotron Resonance Spectrometry", Hartmann, H.; Wanczek, K.-P., Ed.; Springer-Verlag: Berlin, 1978; pp 136–45. White, R. L.; Ledford, E. B., Jr.; Ghaderi, S.; Wilkins, C. L.; Gross, M. L. *Anal. Chem.* **1980**, *52*, 1527–9. Allemann, M.; Kellerhals, Hp.; Wanczek, K.-P. *Chem. Phys. Lett.* **1980**, *75*, 328–31.
(37) McIver, R. T., Jr.; Ledford, E. B., Jr.; Miller, J. S. *Anal. Chem.* **1975**, *47*, 692–7.
(38) Bartmess, J. E.; Caldwell, G., *Int. J. Mass Spectrom. Ion Phys.* **1981**, *40*, 269–74.

Adsorption Kinetics of Ammonia on an Inhomogeneous Gold Surface

R. E. Richton* and L. A. Farrow

Bell Laboratories, Murray Hill, New Jersey 07974 *(Received: March 27, 1981)*

Adsorption kinetics of ammonia onto a gold surface have been studied by monitoring gas concentration as a function of time using the optoacoustic effect. The data can be understood by applying a theory recently formulated by Aharoni and Ungarish which takes into account the inhomogeneity of adsorption energy and site characteristics of a "dirty" surface. If the optoacoustic data are used to obtain the parameters of this theory, differential heat as a function of time can be found. The differential heat of adsorption of ammonia onto gold is found to range from ~2 to ~35 kcal/mol.

Introduction

Experiments in gas-phase kinetics are often complicated by adsorption onto reactor cell surfaces. If such heterogeneous processes between the gas and the wall could be quantitatively predicted, then homogeneous gas-phase rates could more readily be derived from kinetic data. For example, determination of the rate constant for the reaction of nitric acid vapor and ammonia vapor has been complicated by the strong adsorption of these gases onto both wet and dry surfaces.[1] In examining this system by an optoacoustic technique,[2] we found the theory of chem-

(1) K. J. Olszyna, R. G. DePena, and J. Heicklen, *Int. J. Chem. Kinet.*, 8, 357 (1976).

0022-3654/81/2085-3577$01.25/0 © 1981 American Chemical Society